



The photocatalytic degradation of naproxen with g-C₃N₄ and visible light: Identification of primary by-products and mechanism in tap water and ultrapure water

Marta Jiménez-Salcedo^a, Miguel Monge^{a,b}, María Teresa Tena^{a,*}

^a Department of Chemistry, University of La Rioja, C/ Madre de Dios 53, E-26006 Logroño, La Rioja, Spain

^b Centro de Investigación en Síntesis Química (CISQ), University of La Rioja, C/ Madre de Dios 53, E-26006 Logroño, La Rioja, Spain

ARTICLE INFO

Editor: Dr Xianwei Liu

Keywords:

Naproxen
g-C₃N₄ nanosheets
Photocatalysis
Visible light
Tap water
Degradation pathway
By-product formation

ABSTRACT

Differences in the photocatalytic degradation rates of naproxen (a nonsteroidal anti-inflammatory drug) in ultrapure water and tap water were assessed using g-C₃N₄ nanosheets as photocatalyst and irradiating with natural sunlight and low-power (4 × 10 W) white light LEDs. The graphitic carbon nitride (g-C₃N₄) photocatalyst was synthesised and characterised. All the photodegradations followed pseudo-first-order kinetics. Liquid chromatography with tandem mass spectrometry (UPLC-QToF-MS) was used to identify the intermediates generated in the degradation of naproxen by accurate mass and MS/MS data. Among the by-products detected, 2-(naphthalene-2-yl)propanal, a compound with structural warning for genotoxic carcinogenicity, has been reported for the first time. This persistent by-product was completely depleted with g-C₃N₄ and natural sunlight in 50–70 min. According to the kinetics of by-products and spectrometry data a plausible transformation pathway has been proposed. Furthermore, the main active species involved in the photodegradation with g-C₃N₄ were studied to fully understand the process. To accomplish this goal, different scavengers were introduced in the degradation of naproxen to quench possible superoxide radicals ($\cdot\text{O}_2^-$), photoexcited holes (h^+) and hydroxyl radicals ($\cdot\text{OH}$).

1. Introduction

In recent years, the water quality is an issue that has raised serious concerns. The increasing occurrence of pharmaceuticals in the environment due to their extensive use in human and veterinary medicine, is a dreaded environmental problem due to the fact that wastewater treatment plants (WWTPs) are not designed to remove them efficiently [19]. Persistence of pharmaceuticals in the environment itself pose a risk, drugs such as naproxen or sulfamethoxazole can last more than one year in the nature [1]. The presence of pharmaceuticals in aquatic environment could convey a range of adverse effects on aquatic ecosystems or even on the human health.

Non-steroidal anti-inflammatory drugs (NSAIDs) are worldwide prescribed to release pain and fever, being naproxen (NPX) one the most common NSAIDs. The presence of naproxen in different water matrixes (rivers, groundwater, tap water, WWTP influents, etc.) has been reported [2,3,19] in concentrations up to $\mu\text{g/L}$ [2,19,26]. These facts illustrate the great urgency to develop efficient technologies to tackle this issue.

Advanced oxidation processes (AOP), and specifically photocatalysis, has been considered a promising technique to remove emerging water pollutants [25]. Photodegradations are a useful, cheap and non-polluting method to change the bioactive molecule of a pharmaceutical into a non-toxic mixture of by-products [1] because compounds are effectively oxidised. For the remediation of naproxen aquatic pollution, a range of catalytic processes has been reported: photolysis [2], photoelectrocatalysis [3], electro-Fenton treatment [7] or photocatalysis [14,24–26,32].

As a metal-free semiconductor with visible light activity, graphitic carbon nitride (g-C₃N₄) has drawn attention as a photocatalyst for pharmaceuticals remediation in photocatalytic degradation treatments. Their characteristics such as physical and chemical stability or a wide range of precursors for a facile synthesis (dicyanamide, melamine, cyanamide, urea, thiourea or ammonium thiocyanate) [18] make it an ideal material for photocatalysis. In recent years, it has been broadly employed effectively in the removal of several drugs: diclofenac [12,13,16], ciprofloxacin [11,20], ibuprofen [9,10,23], tetracycline [29,33] oxytetracycline [30]. However, for the time being, graphitic carbon

* Corresponding author.

E-mail address: teresa.tena@unirioja.es (M.T. Tena).

<https://doi.org/10.1016/j.jece.2021.106964>

Received 25 June 2021; Received in revised form 19 November 2021; Accepted 4 December 2021

Available online 7 December 2021

2213-3437/© 2021 The Author(s).

Published by Elsevier Ltd.

This is an open access article under the CC BY-NC-ND license

(<http://creativecommons.org/licenses/by-nc-nd/4.0/>).

nitride has been only reported in five studies of photocatalysis of naproxen [24–26,32,6], which illustrates the need for further studies in this field. In this sense, our catalyst stands out for being metal-free, ligand-free and for its structure in nanosheets and for the facile and direct synthesis from the pyrolysis of a single nitrogen-rich precursor, which makes it suitable for real-life applications in water treatment plants.

An important difference between laboratory studies and real-life application is the adopted water matrix. The widespread use of ultrapure water in laboratory tests neglects the effects of electrolytes, minerals and common contaminants in real matrixes. This leads to biased studies when the target is to implement this technology in real-life applications, which in most cases involve real sources of irradiation and real water matrixes. Furthermore, naproxen is frequently excreted metabolised [15], meaning that both naproxen and their metabolites might end up in aquatic environments as water pollutants. Some studies have reported that some of the intermediate products of pharmaceuticals were as toxic as their parents or even more [10,21] for this reason, not only is the depletion of naproxen of utmost importance, but also the study and removal of their intermediates.

In this context, in the present study, the photodegradation of naproxen has been evaluated with g-C₃N₄ nanosheets as photocatalyst in two water matrices (ultrapure water and tap water) and with two sources of irradiation (natural sunlight and low power visible light LED). In addition, three intermediates generated in the degradations have been monitored and analysed by UPLC-QToF-MS, one of them has been reported for the first time. The by-products toxicology has been assessed by Cramer rules. In order to propose a plausible mechanism, the main active species involved in the process were also studied.

2. Experimental

2.1. Materials

Sodium naproxen ($\geq 98\%$) (NPX), tert-butanol and triethanolamine were purchased from Sigma-Aldrich (Germany). Formic acid (98%) for mass spectrometry came from Fluka Analytical. HPLC-grade acetonitrile was obtained from Scharlab (Barcelona, Spain) and melamine (99%) was from Alfa Aesar (Germany). All chemicals were used as received without further purification. Syringe PTFE hydrophilic filters (13 mm, 0.22 μm) were obtained from Proquinorte (Spain).

For photocatalytic degradations studies, solutions of naproxen were prepared in ultrapure water and tap water. The tap water quality parameters are listed in Table S1 (Supplementary material).

2.2. Synthesis and characterisation of g-C₃N₄

The graphitic carbon nitride was synthesised by direct heating of melamine in a covered crucible to prevent sublimation as previously described [12,27]. Briefly, 5 g of melamine were heated first at 500 °C for 4 h, then at 520 °C for 2 h to achieve a thermal oxidative exfoliation. The light absorbance properties and morphology of g-C₃N₄ were characterised by “ERDF A way of making Europe” for financial support transmission electron microscope (TEM) and UV–vis diffuse reflectance spectroscopy of solid samples. Additionally, the stability of the catalyst was evaluated by Fourier transform infrared spectroscopy (FTIR).

2.3. Photocatalytic performance

The degradations of naproxen were performed at natural pH under low power visible light LED and natural sunlight. A lab-made assembly consisting of four 10 W white light LED lamps (LED-Engin, CA, USA) placed equidistantly inside a metal container with circulating coil water to maintain the reactor at a constant temperature of 25 °C was used for the experiments carried out with visible light. Fig. S1 in Supplementary Material shows the relative spectral power vs. wavelength for the LED

visible lamp employed. Whereas experiments with natural sunlight were placed outdoors in summer in the north of Spain, with an average temperature of 30 °C and an ultraviolet index of 7–9, accordingly to the Spanish National Agency of Meteorology reports (www.AMET.es). Table S2 (Supplementary Material) shows specific meteorology data of each experiment and Fig. S2 shows the experimental setup used. Typically, 15 mg of g-C₃N₄ were suspended in 70 mL of 10 mg/L naproxen aqueous solution (ultrapure water or tap water depending on the experiment) in a Schlenk glass reactor. Previously to the irradiation, the solutions were sonicated to disperse properly the catalyst and vigorously stirred for 30 min in dark conditions to establish the adsorption-desorption equilibrium at the surface of the photocatalyst. After that, the mixtures were irradiated (with the corresponding source of light) and continuously stirred. Aliquots were withdrawn at different times to monitor the naproxen depletion and filtered with PTFE hydrophilic filters to remove the catalyst. The samples were stored at 4 °C until analysis.

The identification of intermediates was performed in a naproxen solution in tap water irradiated by natural sunlight. For this experiment the concentration of the solution was 190 mg/L of naproxen and 65 mg of catalyst were added.

2.4. Detection of active species

The role of active species involved in the photocatalytic degradation of naproxen in the system ultrapure water/LED was investigated employing different scavengers to quench the corresponding reactive species. A typical degradation was performed under three different conditions: 10⁻³ M aqueous solution of tert-butanol to quench hydroxyl radicals ($\cdot\text{OH}$) [22,28], 10⁻³ M aqueous solution of triethanolamine to quench photogenerated holes (h^+) [22] and under N₂ atmosphere generated after bubbling N₂ to remove the oxygen in the solution to quench the influence of superoxide radicals ($\cdot\text{O}_2^-$) [8,28]. Indirectly the study of $\cdot\text{O}_2^-$ also imply studying the role of the photoexcited electrons (e^-), since the superoxide radicals are generated from the electrons in the conduction band (CB) of the semiconductor.

2.5. Analytical procedure

Routine analysis of naproxen samples to follow the naproxen depletion and by-products evolution were performed by a high-performance liquid chromatography system. It consists on an Agilent modular 1100/1200 liquid chromatography system (Agilent Technologies, Palo Alto, CA, USA) equipped with a G1379A degasser, a G1311A HPLC quaternary pump, a G1329A autosampler and a G1315D diode array detector. The column used was a Phenomenex Luna® LC C18 100 Å (5 μm particle size, 150 mm \times 4.6 mm i.d.). The mobile phase to achieve a proper separation of by-products was 50/50 of aqueous solution and acetonitrile, both containing 0.1% (v/v) formic acid at a flow-rate of 1.0 mL/min. Injection volume was 20 μL and the separation was performed at room temperature. Detection wavelength was set at 231 nm. All samples were filtered before chromatographic analysis.

The photocatalytic intermediates of naproxen were identified using liquid chromatography with tandem mass spectrometry (UPLC-QToF). This equipment was described in a previous study [10]. A C18 column and a gradient program of mobile phase consisting of aqueous solution and acetonitrile, both containing 0.1% (v/v) formic acid, were employed for the separation. The mass spectra data were obtained in both positive and negative mode and MS/MS data were also recorded for the main signals. The detailed analytical method is conveyed in the Supplementary Material (Text S1).

Finally, the toxicology and carcinogenicity assessments of the naproxen by-products were evaluated employing Toxtree v3.1.0.1851 software according to Cramer rules and mutagenicity rule base by ISS.

3. Results and discussion

3.1. Characterisation of g-C₃N₄

The synthesised graphitic carbon nitride (g-C₃N₄) was characterised by transmission electronic microscopy (TEM) and UV–vis diffuse reflectance. Briefly, Fig. 1 shows the diffuse reflectance UV–vis spectrum, the Tauc plot and a representative TEM image of 2D-nanosheets catalyst displaying a semiconductor band gap of 2.79 eV. Moreover, the band edge positions of conduction band (CB) and valence band (VB) for the semiconductor might be theoretically estimated [4] leading to a valence band edge (E_{VB}) of 1.63 eV and a conduction band edge (E_{CB}) of -1.17 eV according to the equations:

$$E_{VB} = X - E_e + 0.5E_g$$

$$E_{CB} = E_{VB} - E_g$$

where X is the absolute electronegativity of the semiconductor (geometric mean of the absolute electronegativity of the atoms forming the semiconductor: 4.73 for g-C₃N₄); E_e is the energy of the free electrons (ca. 4.5 eV); E_g is the band gap energy of the semiconductor. These values provide information for the explanation of the photocatalytic mechanism and the determination of active species involved in the process.

The stability of the catalyst after the degradation process is relevant for real-life applications. The IR spectrum (Fig. S3) of the catalyst before and after a photocatalytic degradation shows no obvious alterations. The IR spectrum of g-C₃N₄ after degradation shows a broad absorption at ca. 3500 cm⁻¹ arising from adsorbed water. The rest of the spectrum bands: at 820 cm⁻¹ (breathing mode of triazine units) and in the 1100–1700 cm⁻¹ range (strong absorptions assigned to stretching

modes of the CN heterocycles), remained unaltered.

3.2. Photocatalytic degradation of naproxen

The photocatalytic degradation of naproxen with g-C₃N₄ was carried out under low power visible light and natural sunlight in both ultrapure and tap water in order to compare the effect of different water matrices and irradiation sources for this photocatalyst. As it is shown in Fig. 2a, the degradation of naproxen in the absence of photocatalyst (photolysis) was negligible in both water matrices when the irradiation source was low power LED light. Whereas with a more powerful irradiation source, natural sunlight (Fig. 2b), a total degradation was achieved by photolysis after less than 80 min of solar light exposure. After 30 min of stirring and reaching the adsorption-desorption equilibrium, the adsorption of pharmaceutical on the surface of g-C₃N₄ was around 1% for both types of water matrices, which illustrated that in this case the water matrix has no influence in the interaction between naproxen and g-C₃N₄.

When the samples were irradiated with visible LED light (Fig. 2a), total depletion of naproxen was achieved using g-C₃N₄ in less than 85 and 110 min in tap water and ultrapure water, respectively. The pseudo-first-order kinetic constants were 0.048 and 0.081 min⁻¹ for ultrapure water and tap water, respectively. Moreover, the photocatalytic degradation showed a remarkable enhancement in tap water. Wang et al. [25] observed the same effect in tap water naproxen degradations and carried out several degradation studies with solutions containing different inorganic anions, cations and organic matter to elucidate this fact. They concluded that the presence of divalent cations (Mg²⁺ and Ca²⁺) enhanced the depletion efficiency. Other authors also observed higher removal rates in tap water with several pollutants [5,17]. Nieto-Sandoval et al. ascribed this fact to the presence of chloride ions of salts. However, Wang et al. did not observe the chloride influence on the

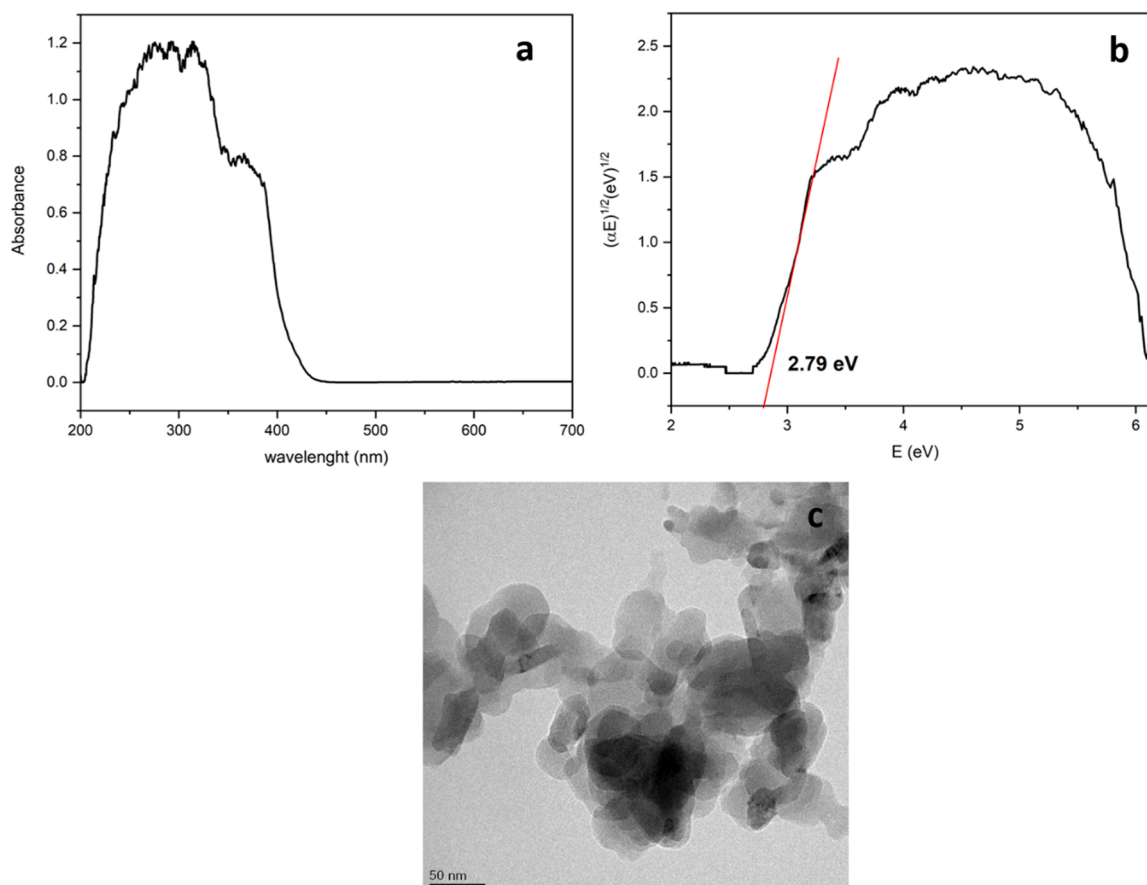


Fig. 1. Diffuse reflectance UV-Vis spectrum of g-C₃N₄ solid samples (a). Tauc plot for g-C₃N₄ (b). TEM images of g-C₃N₄ (c).

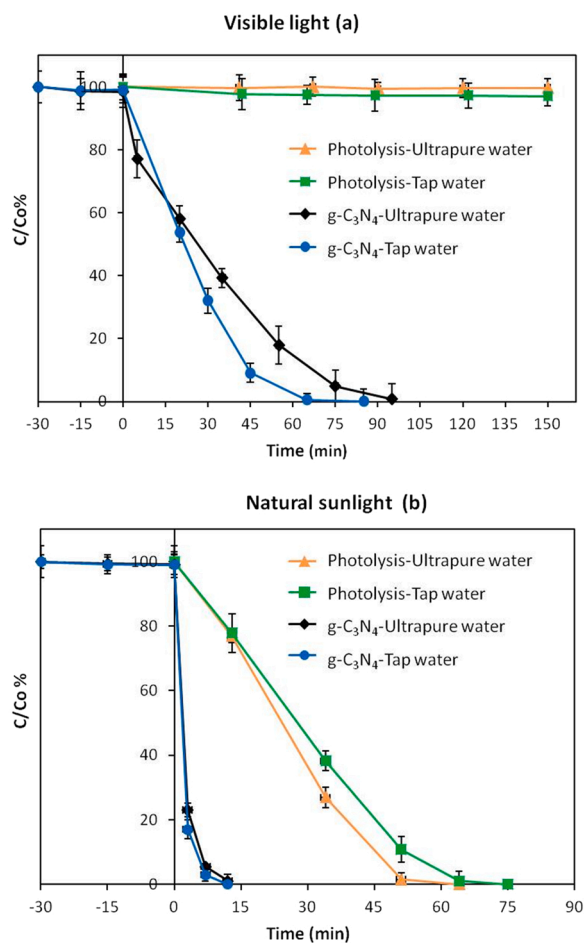


Fig. 2. Photocatalytic degradation of naproxen with g-C₃N₄ and visible light radiation (a) and natural sunlight (b).

photocatalytic degradation of naproxen.

On the other hand, when samples were irradiated with natural sunlight in the presence of g-C₃N₄, naproxen was totally removed after approximately 10 min, and the removal efficiency was around 98% after 8 min in both water matrices. In this case, slight differences were observed in tap and ultrapure water with pseudo-first-order kinetic constants of 0.43 and 0.36 min⁻¹, respectively. The difference between the two water matrices was not as noticeable as it was in visible-light experiments probably due to the faster naproxen removal with sunlight. The statistical data about kinetics and regression graphs are summarised in the [Supplementary Material \(Table S3 and Fig. S4\)](#).

The pseudo-first-order kinetic constants obtained in experiments with natural sunlight were meaningfully higher than those with visible light LEDs as expected, especially considering the nature of the two sources of light employed for the irradiation. Visible light LED is not nearly as powerful as natural sunlight, in addition to the fact that natural sunlight radiation also presents an important percentage of ultraviolet and infrared light. Wu et al. [26] also observed fast depletion of naproxen with a more complex catalyst (carbon dots/g-C₃N₄ nanospheres) and natural sunlight, achieving complete naproxen removal within 5 min

3.3. Reactive species

The naproxen degradation is caused by reactive oxygen species formed during the photocatalytic degradation process. To confirm the photocatalytic mechanism and identify which species is involved in the process, three trapping experiments were carried out in ultrapure water

with visible light. Fig. 3 shows the influence of hydroxyl radicals ($\cdot\text{OH}$), photogenerated holes (h^+) and superoxide radicals ($\cdot\text{O}_2^-$) on the photodegradation of naproxen. The depletion rates were almost totally inhibited with the addition of triethanolamine and partially inhibited under inert atmosphere conditions. On the contrary, the addition of tert-butanol had a negligible effect on the degradation. Consequently, the photogenerated holes and superoxide radicals were the main species in the photocatalytic mechanism, whereas hydroxyl radicals were not involved in the mechanism, or at least not significantly. These results agree with previous reports of different catalytic systems based on g-C₃N₄ [4,12,31]. The conduction band (CB) edge of g-C₃N₄ is more negative (-1.17 eV, vs. NHE) than the formation potential of superoxide radicals $\text{O}_2/\cdot\text{O}_2^-$ (-0.33 eV, vs. NHE) and, therefore, the photoexcited electrons on the CB can reduce the O_2 .

3.4. Identification of naproxen intermediate products

The study of naproxen intermediates was carried out in a naproxen tap water solution irradiated with natural sunlight. The chromatogram of the degraded solution showed four peaks: three by-products eluted at 2.46, 3.08 and 4.00 min (hereinafter referred as P1, P2 and P3, respectively) and the naproxen peak eluted at 2.78 min Fig. S5 depicts a typical chromatogram recorded in positive and negative ESI modes and with UV detector at 231 nm. The only compound detected in negative mode was naproxen. Table 1 summarises the MS data: main m/z signals of the ions detected for each peak, the elementary composition of these ions, the mass errors and the fragment ions found in MS² experiments. Furthermore, Table 2 contents the structures proposed for the by-products and the MS and MS² spectra are shown in Figs. S6 and S7, respectively.

The first by-product, P1, was eluted at 2.46 min with a main signal at m/z 185.0969 in the +MS spectrum. This signal was assigned to the protonated ion of a by-product with formula C₁₃H₁₂O (error 3.2 ppm): 2-(naphthalen-2-yl)propanal, which is reported as a naproxen photo-degradation by-product for the first time. The MS² spectrum shows three main signals at m/z 169 (C₁₂H₉O⁺), 152 (C₁₂H₈⁺) and 141 (C₁₁H₉⁺) that support the structure proposed for P1. The structures proposed for the MS² fragments are depicted in Fig. S7.

Naproxen was the next peak in the chromatogram, eluting at 2.78 min. Its protonated and sodiated ions at m/z 231.1018 and 253.0836, respectively were measured with errors of 0.2 and -0.4 ppm, respectively.

The intermediate P2 presents a main signal at m/z 201.0916 and a small signal at m/z 223.0722 assigned to the protonated and the sodiated ions corresponding to a compound with formula C₁₃H₁₂O₂. Two isomers could fit that formula, a ketone or an aldehyde, however the

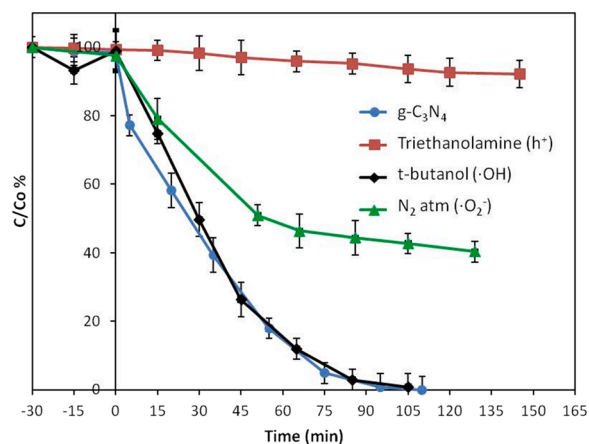
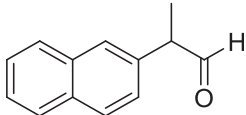
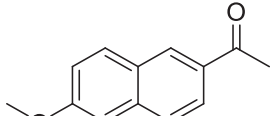
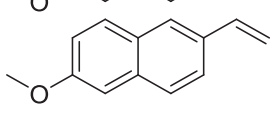


Fig. 3. Effect of different scavengers on the photodegradation of naproxen with g-C₃N₄ under visible light.

Table 1
Summary of UPLC-ESI-MS and MS² results for naproxen photodegradation with tap water/g-C₃N₄/sunlight.

t _R , min	Experimental mass m/z	Ion	Elementary composition	Error (× 10 ⁻⁶)	Compound formula	MS ² Fragments
2.46 (P1)	185.0969	[M+H] ⁺	C ₁₃ H ₁₃ O ⁺	3.2	C ₁₃ H ₁₂ O	141.0758 (C ₁₁ H ₉ ⁺) 152.0687 (C ₁₂ H ₈ ⁺) 169.0725 (C ₁₂ H ₉ O ⁺)
2.78 (NPX)	231.1018	[M+H] ⁺	C ₁₄ H ₁₅ O ₃ ⁺	0.2	C ₁₄ H ₁₄ O ₃	153.0762 (C ₁₂ H ₉ ⁺) 185.1037 (C ₁₃ H ₁₃ O ⁺)
3.08 (P2)	253.0836 201.0916	[M+Na] ⁺ [M+H] ⁺	C ₁₄ H ₁₄ O ₃ Na ⁺ C ₁₃ H ₁₃ O ₂ ⁺	-0.4 1.8	C ₁₃ H ₁₂ O ₂	144.0620 (C ₁₀ H ₈ O ⁺) 155.0670 (C ₁₁ H ₇ O ⁺)
4.00 (P3)	223.0722 185.0963	[M+Na] ⁺ [M+H] ⁺	C ₁₃ H ₁₂ O ₂ Na ⁺ C ₁₃ H ₁₃ O ⁺	-4.5 -0.1	C ₁₃ H ₁₂ O	141.0747 (C ₁₁ H ₉ ⁺) 152.0668 (C ₁₂ H ₈ ⁺) 169.0690 (C ₁₂ H ₉ O ⁺)

Table 2
Proposed identification of naproxen photodegradation by-products.

Compound formula	Chemical structure proposed	Name	Structure reported in
C ₁₃ H ₁₂ O ₂ P1		2-(naphthalen-2-yl)propanal	-
C ₁₃ H ₁₂ O ₂ P2		1-(6-methoxynaphthalen-2-yl)ethan-1-one	[2] [24] [15] [26] [25] [32]
C ₁₃ H ₁₂ O ₂ P3		2-methoxy-6-vinylnaphthalene	[2] [14] [24] [15] [26] [25] [3] [32]

MS² data confirmed the structure: 1-(6-methoxynaphthalen-2-yl)ethan-1-one (see Table 2). The MS² spectrum of the ion 201 shows two signals at m/z 144 and 155 that were essential for the elucidation of the structure. The fragment proposed for the signal m/z 155 confirms that the structure should be the ketone and not the aldehyde 2-(6-methoxynaphthalen-2-yl)acetaldehyde. This compound was also reported previously by other authors (see Table 2), however only two of these works provided MS² data, but they did not discuss the structure of the fragment ions. Wu et al. [26] detected fragment ions at m/z 144 and 159, whereas Wang et al. [24] only found the ion m/z 159, which was not detected in this work.

The last by-product detected was eluted at 4.00 min and presents a main signal in the positive MS spectrum at m/z 185.0963 assigned to the protonated ion C₁₃H₁₃O⁺ (error -0.1 ppm). This ion was also detected in P1, subsequently, P1 and P3 are isomers (see Table 2). P3 was assigned to 2-methoxy-6-vinylnaphthalene. The main signals in the MS² spectrum were detected at m/z 141 (C₁₁H₉⁺), 152 (C₁₂H₈⁺) and 169 (C₁₂H₉O⁺) and the corresponding structures are shown in Fig. S6. This compound results from the naproxen decarboxylation and it has been reported in previous works with different catalytic systems: photolysis [2,15], photocatalysis with g-C₃N₄ [24–26,32], photocatalysis with TiO₂ [14], photoelectrocatalysis [3]. Wu et al. [26] also detected the m/z fragment 169 in the MS² spectrum among others, while Wang et al. [24] detected the MS² ions 179, 170, 153 and 57, however none of them proposed a plausible structure or formula for these fragments.

In the assignment of the proposed structures for C₁₃H₁₂O isomers detected (P1 and P3), the polarity of the molecules was the key. The most polar molecule should elute the first in a reverse-phase partitioning chromatography. Therefore, the 2-(naphthalen-2-yl)propanal was

assigned to P1. This aldehyde which is in equilibrium with its corresponding enol tautomer, is more polar than the ether 2-methoxy-6-vinylnaphthalene and therefore it is less retained in the C18 column.

The toxicity and carcinogenicity of these compounds was determined with the Toxtree software. The three by-products and the naproxen were classified as high toxic hazard (Class III) according to Cramer rules. Additionally, P1 shows a structural alert for genotoxic carcinogenicity.

3.5. Degradation mechanism and pathway

The naproxen degradation mechanism was ascribed to the action of holes (h⁺) and superoxide radicals (·O₂⁻) as it was confirmed with the scavenger's tests. This agrees with the structure proposed for the by-products. None of them seems to derive from the attack of hydroxyl radicals to naproxen as it has been reported [24–26]. Fig. 4 shows a plausible mechanism proposed to the naproxen degradation and by-products formation.

Naproxen seems to be degraded following two routes. On one hand, naproxen is attacked by holes at alpha carbon resulting in decarboxylation and the formation of a radical that can be attacked again by holes to form P3 or react with superoxide radicals to produce P2. On the other hand, P1 is formed by the loss of the methoxy group after h⁺ attack and the simultaneous attack to the carboxylic carbon by photoexcited electrons. As a result, the carboxylic acid is reduced to an aldehyde.

Furthermore, Fig. S8 shows the formation and evolution of the by-products in the two water matrices studied and with the two sources of irradiation. In the degradations carried out with visible LED light, the three by-products (P1, P2 and P3) were detected and they followed the same evolution regardless of the type of water. In ultrapure water, P2

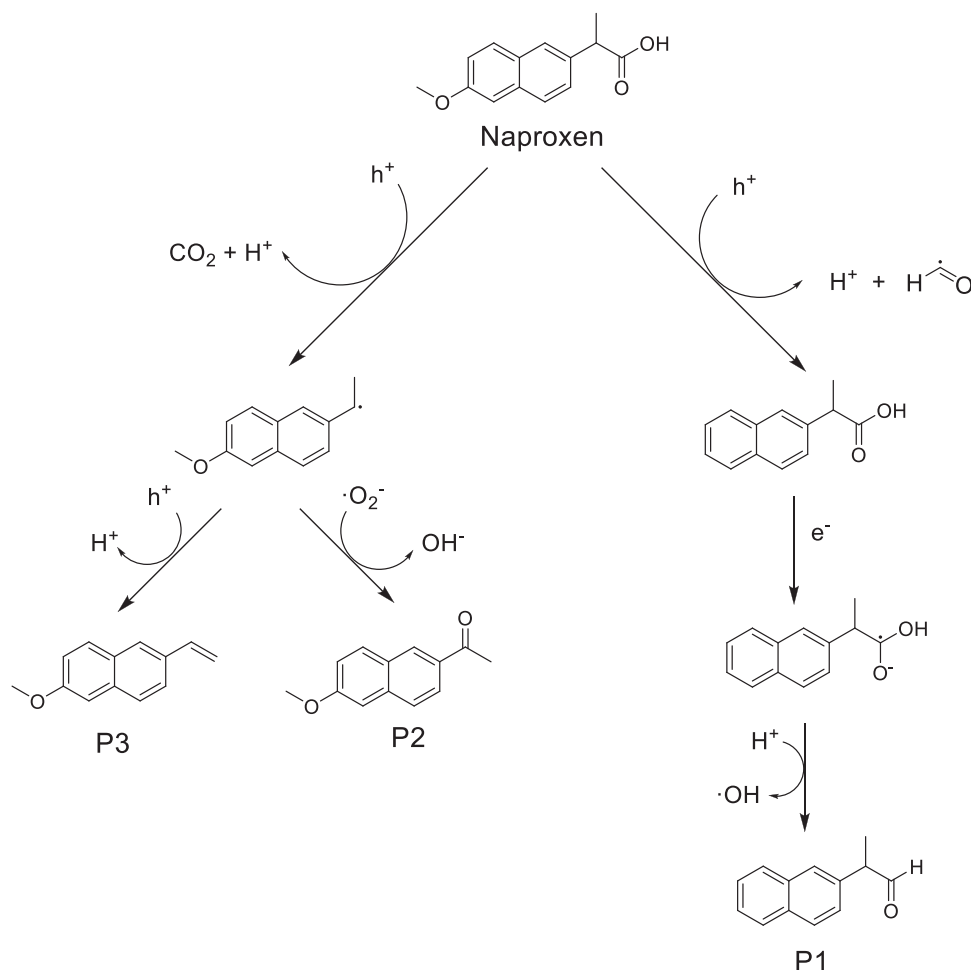


Fig. 4. Proposed photodegradation pathway for naproxen with $g\text{-C}_3\text{N}_4$ nanosheets.

was formed and totally degraded in 110 min, whereas in tap water this process only involved 65 min. P1 and P3 were persistent by-products, they were not depleted in tap water even after 350 min of irradiation. With natural sunlight, only P1 and P3 were detected and almost totally degraded in 50 and 70 min in ultrapure water and tap water, respectively.

4. Conclusions

In this work, total photodegradation of naproxen with a visible-light driven photocatalyst ($g\text{-C}_3\text{N}_4$) was accomplished with natural sunlight and visible LED light. Degradations in tap water exhibited higher removal efficiency than degradations in ultrapure water, achieving the complete naproxen depletion in less than 12 min in tap water with natural sunlight and a pseudo-first-order kinetic constant of 0.43 min^{-1} .

Three by-products have been tentatively identified by UPLC-QToF-MS and one of them has been reported for the first time (2-(naphthalen-2-yl)propanal). Moreover, the chemical structure proposals were supported by MS² data and the by-products evolution was monitored by HPLC-UV. The three by-products detected, as well as naproxen, were found high toxic hazard (Class III) according with Cramer rules.

Photogenerated holes and superoxide radicals were the main reactive species involved in the naproxen photodegradation with $g\text{-C}_3\text{N}_4$. Two routes are proposed for naproxen degradation. In the first pathway, the alpha carbon of naproxen is attacked by holes followed by decarboxylation. Then, the resulting radical intermediate might react with another hole to produce 2-methoxy-6-vinylnaphthalene or with a superoxide radical to form 1-(6-methoxynaphthalen-2-yl)ethan-1-one. The

second pathway gives rise to 2-(naphthalen-2-yl)propanal as a result of loss of the methoxy group by the attack of photogenerated holes and the reduction of the carboxylic acid by photoexcited electrons.

CRedit authorship contribution statement

Marta Jiménez-Salcedo: Investigation, Visualization, Writing – original draft. **Miguel Monge:** Project administration, Funding acquisition, Conceptualization, Supervision, Writing – review & editing (Catalyst synthesis and characterisation). **María Teresa Tena:** Conceptualization, Supervision, Writing – review & editing (Mass spectrometry and kinetics).

Declaration of Competing Interest

The authors declare that they have no known competing financial interests or personal relationships that could have appeared to influence the work reported in this paper.

Acknowledgements

We thank the Grant PID2019-104379RB-C22 funded by MCIN/AEI/10.13039/501100011033 and by “ERDF A way of making Europe” for financial support. And the University of La Rioja (Spain) for the financing of the M.Jiménez-Salcedo’s predoctoral grant.

Appendix A. Supporting information

Supplementary data associated with this article can be found in the online version at [doi:10.1016/j.jece.2021.106964](https://doi.org/10.1016/j.jece.2021.106964).

References

- [1] S. Andini, A. Bolognese, D. Formisano, M. Manfra, F. Montagnaro, L. Santoro, Mechanochemistry of ibuprofen pharmaceutical, *Chemosphere* 88 (2012) 548–553.
- [2] E. Arany, R.K. Szabol, L. Apáti, T. Alapi, I. Ilisz, P. Mazellier, A. Dombi, K. Gajda-Schranz, Degradation of naproxen by UV, VUV photolysis and their combination, *J. Hazard. Mater.* 262 (2013) 151–157.
- [3] K. Changanaqui, H. Alarcón, E. Brillas, I. Sirés, Blue LED light-driven photoelectrocatalytic removal of naproxen from water: Kinetics and primary by-products, *J. Electroanal. Chem.* 867 (2020), 114192.
- [4] S. Chen, Y. Hu, S. Meng, X. Fu, Study on the separation mechanisms of photogenerated electrons and holes for composite photocatalyst g-C₃N₄-WO₃, *Appl. Catal. B: Environ.* 150–151 (2014) 564–573.
- [5] P. Chen, Q. Zhang, L. Shen, R. Li, C. Tan, T. Chen, H. Liu, Y. Liu, Z. Cai, G. Liu, W. Lv, Insights into the synergetic mechanism of a combined vis-RGO/TiO₂/peroxodisulfate system for the degradation of PPCPs: Kinetics, environmental factors and products, *Chemosphere* 216 (2019) 341–351.
- [6] K. Fu, Y. Pan, C. Ding, J. Shi, H. Deng, Photocatalytic degradation of naproxen by Bi₂MoO₆/g-C₃N₄ heterojunction photocatalyst under visible light: mechanisms, degradation pathway, and DFT calculation, *J. Photochem. Photobiol. A: Chem.* 412 (2021), 113235.
- [7] O. Ganzenko, C. Trelu, N. Oturan, D. Huguenot, Y. Péchaud, E.D. Hullebusch, M. A. Oturan, Electro-Fenton treatment of a complex pharmaceutical mixture: Mineralization efficiency and biodegradability enhancement, *Chemosphere* 253 (2020), 126659.
- [8] R. Hao, G. Wang, H. Tang, L. Sun, C. Xu, D. Han, Template-free preparation of macro/mesoporous g-C₃N₄/TiO₂ heterojunction photocatalysts with enhanced visible light photocatalytic activity, *Appl. Catal. B: Environ.* 187 (2016) 47–58.
- [9] D.B. Hernández-Uresti, A. Vázquez, D. Sánchez-Martínez, S. Obregón, Performance of the polymeric g-C₃N₄ photocatalyst through the degradation of pharmaceutical pollutants under UV–vis irradiation, *J. Photochem. Photobiol. A: Chem.* 324 (2016) 47–52.
- [10] M. Jiménez-Salcedo, M. Monge, M.T. Tena, Photocatalytic degradation of ibuprofen in water using TiO₂/UV and g-C₃N₄/visible light: study of intermediate degradation products by liquid chromatography coupled to high-resolution mass spectrometry, *Chemosphere* 215 (2019) 605–618.
- [11] M. Jiménez-Salcedo, M. Monge, M.T. Tena, Study of intermediate by-products and mechanism of the photocatalytic degradation of ciprofloxacin in water using graphitized carbon nitride nanosheets, *Chemosphere* 247 (2020), 125910.
- [12] M. Jiménez-Salcedo, M. Monge, M.T. Tena, The photocatalytic degradation of sodium diclofenac in different water matrices using g-C₃N₄ nanosheets: a study of the intermediate by-products and mechanism, *J. Environ. Chem. Eng.* 9 (2021), 105827.
- [13] X. Jin, Y. Wu, Q. Zhang, F. Wang, P. Chen, H. Liu, S. Huang, J. Wu, N. Tu, W. Lv, G. Liu, Defect-modified reduced graphitic carbon nitride (RCN) enhanced oxidation performance for photocatalytic degradation of diclofenac, *Chemosphere* 258 (2020), 127343.
- [14] D. Kanakaraju, C.A. Motti, B.D. Glass, M. Oelgemöller, TiO₂ photocatalysis of naproxen: Effect of the water matrix, anions and diclofenac on degradation rates, *Chemosphere* 135 (2015) 579–588.
- [15] D. Krakkó, E. Gombos, V. Licul-Kucera, S. Dóbbé, G.V. Mihucz, G. Záray, Enhanced photolytic and photooxidative treatments for removal of selected pharmaceutical ingredients and their degradation products in water matrices, *Microchem. J.* 150 (2019), 104136.
- [16] W. Liu, Y. Li, F. Liu, W. Jiang, D. Zhang, J. Liang, Visible-light-driven photocatalytic degradation of diclofenac by carbon quantum dots modified porous g-C₃N₄: mechanisms, degradation pathway and DFT calculation, *Water Res.* 151 (2019) 8–19.
- [17] J. Nieto-Sandoval, M. Muñoz, Z.M. de Pedro, J.A. Casas, Catalytic hydrodechlorination as polishing step in drinking water treatment for the removal of chlorinated micropollutants, *Sep. Purif. Technol.* 227 (2019), 115717.
- [18] W.-J. Ong, L.-L. Tan, Y.H. Ng, S.-T. Yong, S.-P. Chai, Graphitic carbon nitride (g-C₃N₄)-based photocatalysts for artificial photosynthesis and environmental remediation: are we a step closer to achieving sustainability? *Chem. Rev.* 116 (2016) 7159–7329.
- [19] M. Patel, R. Kumar, K. Kishor, T. Mlsna, C.U. Pittman Jr., D. Mohan, Pharmaceuticals of emerging concern in aquatic systems: chemistry, occurrence, effects, and removal methods, *Chem. Rev.* 119 (2019) 3510–3673.
- [20] S.P. Pattnaik, A. Behera, S. Martha, R. Acharya, K. Parida, Facile synthesis of exfoliated graphitic carbon nitride for photocatalytic degradation of ciprofloxacin under solar irradiation, *J. Mater. Sci.* 54 (2019) 5726–5742.
- [21] H. Tian, Y. Fan, Y. Zhao, L. Liu, Elimination of ibuprofen and its relative photoinduced toxicity by mesoporous BiOBr under simulated solar light irradiation, *RSC Adv.* 4 (2014) 13061.
- [22] H. Wang, J. Li, C. Ma, Q. Guan, Z. Lu, P. Huo, Y. Yan, Melamine modified P25 with heating method and enhanced the photocatalytic activity on degradation of ciprofloxacin, *Appl. Surf. Sci.* 329 (2015) 17–22.
- [23] J. Wang, L. Tang, G. Zeng, Y. Deng, Y. Liu, L. Wang, Y. Zhou, Z. Guo, J. Wang, C. Zhang, Atomic scale g-C₃N₄/Bi₂WO₆ 2D/2D heterojunction with enhanced photocatalytic degradation of ibuprofen under visible light irradiation, *Appl. Catal. B: Environ.* 209 (2017) 285–294.
- [24] F. Wang, Y. Wang, Y. Feng, Y. Zeng, Z. Xie, Q. Zhang, Y. Su, P. Chen, Y. Liu, K. Yao, W. Lv, G. Liu, Novel ternary photocatalyst of single atom-dispersed silver and carbon quantum dots co-loaded with ultrathin g-C₃N₄ for broad spectrum photocatalytic degradation of naproxen, *Appl. Catal. B: Environ.* 221 (2018) 510–520.
- [25] Y. Wang, B. Jing, F. Wang, S. Wang, X. Liu, Z. Ao, C. Li, Mechanism Insight into enhanced photodegradation of pharmaceuticals and personal care products in natural water matrix over crystalline graphitic carbon nitrides, *Water Res.* 180 (2020), 115925.
- [26] Y. Wu, F. Wang, X. Jin, X. Zheng, Y. Wang, D. Wei, Q. Zhang, Y. Feng, Z. Xie, P. Chen, H. Liu, G. Liu, Highly active metal-free carbon dots/g-C₃N₄ hollow porous nanospheres for solar-light-driven PPCPs remediation: Mechanism insights, kinetics and effects of natural water matrices, *Water Res.* 172 (2020), 115492.
- [27] S.C. Yan, Z.S. Li, Z.G. Zou, Photodegradation performance of g-C₃N₄ fabricated by directly heating melamine, *Langmuir* 25 (2009) 10397–10401.
- [28] Z. Yang, J. Yan, J. Lian, H. Xu, X. She, H. Li, g-C₃N₄/TiO₂ Nanocomposites for degradation of ciprofloxacin under visible light irradiation, *Chem. Sel.* 1 (2016) 5679–5685.
- [29] Y. Yang, G. Zeng, D. Huang, C. Zhang, D. He, C. Zhou, W. Wang, Xiong, B. Song, H. Yi, S. Ye, X. Ren, In situ grown single-atom cobalt on polymeric carbon nitride with bidentate ligand for efficient photocatalytic degradation of refractory antibiotics, *Small* 16 (2020), 2001634.
- [30] Y. Yang, G. Zeng, D. Huang, C. Zhang, D. He, C. Zhou, W. Wang, W. Xiong, X. Li, B. Li, W. Dong, Y. Zhou, Molecular engineering of polymeric carbon nitride for highly efficient photocatalytic oxytetracycline degradation and H₂O₂ production, *Appl. Catal. B: Environ.* 272 (2020), 118970.
- [31] W. Zhang, L. Zhou, J. Shi, H. Deng, Fabrication of novel visible-light-driven AgI/g-C₃N₄ composites with enhanced visible-light photocatalytic activity for diclofenac degradation, *J. Colloid Interface Sci.* 496 (2017) 167–176.
- [32] Z. Zhao, W. Zhang, W. Liu, Y. Li, J. Ye, J. Liang, M. Tong, Single-atom silver induced amorphization of hollow tubular g-C₃N₄ for enhanced visible light-driven photocatalytic degradation of naproxen, *Sci. Total Environ.* 742 (2020), 140642.
- [33] Y. Zhou, C. Zhang, D. Huang, W. Wang, Y. Zhai, Q. Liang, Y. Yang, S. Tian, H. Luo, D. Qin, Structure defined 2D Mo₂C/2Dg-C₃N₄ Van der Waals heterojunction: oriented charge flow in-plane and separation within the interface to collectively promote photocatalytic degradation of pharmaceutical and personal care products, *Appl. Catal. B: Environ.* 301 (2022), 120749.